Journal of New Materials for Electrochemical Systems 21, 043-049 (2018)

Study of Ethanol Electrooxidation Reaction at Room Temperature on Nanometric Pt-Ru, Pt-Sn and Pt-Ru-Sn in Direct Alcohol Fuel Cells

F.Ginez Carbajal[1], M.A. García[1] and S.A. Gamboa[2,*]

[1]Universidad Politécnica del Estado de Guerrero. Carretera Federal Iguala-Taxco Km 105 Puente Campuzano, 40321. Taxco de Alarcón Guerrero, México.

[2]Instituto de Energías Renovables, Universidad Nacional Autónoma de México. Privada Xochicalco s/n, Centro, 62580, Temixco, Morelos, México.

Received: October 17, 2017, Accepted: January 22, 2018, Available online: April 17, 2018

Abstract: *Ethanol electrooxidation in acid medium was investigated on Pt-Ru-Sn/C, Pt-Ru/C and Pt-Sn/C. The electrocatalysts were synthesized by microwave assisted chemical reduction reaction. The samples were characterized by transmission electron microscopy (TEM), X-ray diffraction analysis (XRD) and electrochemical analysis for the electrooxidation of ethanol. The ternary electrocatalyst was evaluated in an experimental Direct Ethanol Fuel Cell (DEFC). The method of synthesis used in this work allowed the formation of nanostructured electrocatalysts. The results obtained by electrochemical studies showed that the ternary system Pt-Ru-Sn/C exhibited the highest activity with respect to the binary systems Pt-Ru/C and Pt-Sn/C for carrying out the ethanol electrooxidation reaction. 0.4 mg·cm^{-2} of electrocatalytic load of Pt-Ru-Sn/C was placed in the anode of an experimental fuel cell operating at room temperature. It was possible to obtain a power density of 0.14, 0.12 and 0.11 mW·cm^{-2} after 20, 40 and 60 minutes respectively. The experiments were carried out at a controlled temperature of 297 K and they showed the feasibility to produce electricity at room temperature by using this ternary electrocatalyst in Direct Ethanol Fuel Cells.*

Keywords: Nanostructured Electrocatalyst, Pt-Ru-Sn/C, Ethanol electrooxidation, Direct Ethanol Fuel Cell.

1. INTRODUCTION

Fuel cells are interesting systems because they convert directly any energetic vector as hydrogen or alcohol into electricity. Direct Alcohol fuel cells (DAFC) have attracted the attention due to the possibility to use low molecular weight alcohols for producing electricity for portable electronic devices [1]. The proposed alcohols for operating DAFCs are methanol, ethanol, propanol and butanol [2-3]. The general equation for alcohol electrooxidation can be written as follows:

$$C_nH_{2n+1}OH + (2n-1)\ H_2O \rightarrow (n)\ CO_2 + (6n)\ H^+ + (6n)\ e^- \quad (1)$$

where (n) represents the number of carbon atoms forming the alcohol.

According to eq. (1), the complete electrooxidation of alcohol requires multi-step processes, affecting the kinetic velocity and the performance of a DAFC. During the electrooxidation reaction, there occurs the adsorption of some intermediate species on the surface of the electrocatalytic material, poisoning the main electrocatalyst, in this case: Pt.

Ethanol shows promising characteristics for being considered as a sustainable fuel of the future, especially when it could be used in DAFCs. Ethanol is a very low toxic material, environmentally friendly and the most important: it can be produced from biomass. The complete electrooxidation reaction of ethanol involves the separation of a C-C bond promoting the electronic transfer of 12 electrons. The production of 12 electrons in ethanol electrooxidation is a more complex reaction than methanol electrooxidation, and it is the most interesting challenge of the actual research for developing catalytic materials to be used in the anode of Direct Ethanol Fuel Cells. It is necessary to develop new and very active electrocatalysts to complete the ethanol electrooxidation reaction, diminishing the adsorption of intermediate species [4]. There are relevant works reported in literature about the development of

*To whom correspondence should be addressed: Email: sags@ier.unam.mx
Phone: +52-55-56229706

bimetallic or multi-metallic based electrocatalysts for their potential use in direct ethanol fuel cells, where Pt is still the main electrocatalyst and the operating temperature of the DEFCs is about 350 K. Some examples of those materials are: Pt-Ru [5], Pt-Sn [6], Pt-Rh [7], Pt-Au [8], Pt-Mo y Pt-W [9], Pt-Pd [10], Pt-Au-Sn [4], Pt-Cr-Co [11], Pt-Ru-Rh [12], Pt-Ru-Mo [13], Pt-Sn-Ni and Pt-Sn-Rh [1]. In this work, metallic nanoparticles based on Pt-Ru, Pt-Sn and Pt-Ru-Sn were synthesized by microwave assisted alcohol-reduction method, where the solvent was used at the same time as the reducing agent. Carbon Vulcan XC-72R was used as the supporting material of all synthesized electrocatalysts. The supported electrocatalysts based on Pt-Ru/C, Pt-Sn/C and Pt-Ru-Sn/C, were characterized by XRD, TEM, cyclic voltammetry, Electrochemical Impedance Spectroscopy (EIS) and chronoamperometry. The ternary electrocatalyst was evaluated in an experimental DEFC operating at room temperature.

2. EXPERIMENTAL

2.1. Preparation of electrocatalysts

The metallic precursors were chloroplatinic acid hydrate ($H_2PtCl_6 \cdot xH_2O$), ruthenium chloride hydrate ($RuCl_3 \cdot xH_2O$) and tin chloride dihydrate ($SnCl_2 \cdot 2H_2O$), the chemicals were reagent grade (Aldrich). A mixture of ethanol/deionized-water was used as solvent (4:1 v/v). The molar ratio of dissolved metals (Pt:Ru:Sn) was 1:1:1. The same molar ratio was used to prepare the bimetallic electrocatalysts Pt-Sn and Pt-Ru. The electrocatalysts were synthesized using a modified method based on alcohol-reduction process [14-16] but assisted by microwave heating [4, 17]. The solvent was used as the reducing agent and there was not necessary the addition of any stabilizing material due to the fast synthesis process used in this work for the synthesis of nanoparticles. The metallic ions of Pt, Sn and Ru were reduced at one-step synthesis to obtain the binary or ternary electrocatalytic systems. 5.0 mM of every metallic salt was mixed in a reaction volume of 20 mL. The solution containing two or three dissolved salts at equal proportion was introduced in the microwave reactor (Synthos 3000, AntonPaar) for 5 min at 368 K. After the irradiation by microwaves, a black powder was obtained and it was washed with deionized water on a membrane filter. The electrocatalytic powders were dried at 363 K for 3 hr under nitrogen atmosphere.

2.2. Preparation of the working electrode

Carbon Vulcan XC-72R was used as supporting material to obtain Pt-Ru-Sn/C, Pt-Ru/C and Pt-Sn/C. The supporting process of electrocatalysts on carbon involved the oxidation of carbon by immersion in H_2O_2 at 5% v/v for 5 min at a temperature ca. 353 K. It is a simple activation process widely used to create functional groups on the surface of the carbon to anchor metallic nanoparticles. Supported electrocatalysts were obtained *in situ* during the formation of the electrocatalytic inks. They were prepared by adding 1 mg of binary or ternary electrocatalysts and 4 mg of oxidized carbon in 20 μL of 2-propanol, containing 1.5 μL of liquid Nafion (5 wt.% with respect to aliphatic alcohols). The suspensions were placed in an ultrasonic bath for 30 min to obtain the electrocatalytic inks of Pt-Ru/C, Pt-Sn/C and Pt-Ru-Sn/C. 2 μL of every electrocatalytic ink was placed on the circular surface (0.07 cm^2) of a cylindrical vitreous carbon that was forming the rotating disk electrode of an electrochemical cell. In every experiment, the ink was carefully dried at room temperature maintaining a laminar film on the surface of the electrode.

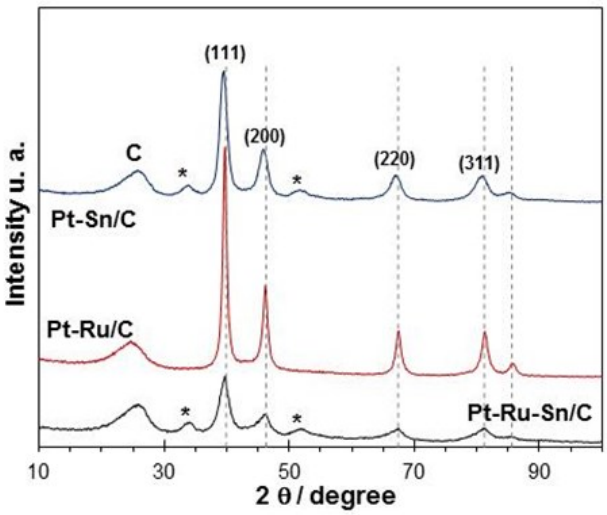

Figure 1. XRD patterns of Pt-Sn/C, Pt-Ru/C and Pt-Ru-Sn/C supported electrocatalysts, with the presence of SnO_2 planes (*).

2.3. Structural and electrochemical characterization

X-ray diffraction patterns were obtained by analyzing the samples in a Rigaku Diffractometer DMAX 2200 with radiation source CuKá (λ = 0.15406 nm). The experiments were carried out in 2θ region from 10° to 100°, step = 1.0°·s^{-1}. Particle size distribution was analyzed by TEM in a JEOL model 2200FS at 200 kV.

The electrochemical characterization was performed by cyclic voltammetry, chronoamperometry and electrochemical impedance spectroscopy in a three-compartment electrochemical cell. The electrolyte for the electrochemical experiments was 0.5 M sulfuric acid + 1.0 M ethanol. A graphite rod and a mercury/mercury sulphate electrode ($Hg/Hg2SO_4$) were used as counter electrode and reference potential respectively. The potentials reported in this work were normalized with respect to the normal hydrogen electrode (NHE). The electrochemical measurements were carried out in a Solartron potentiostat/galvanostat (SI1287) using CorrWare and Zplot software for impedance analysis. In this case, the imposed a.c. signal was 5 mV and the frequency range was from 1 mHz to 500 KHz.

The performance of Pt-Ru-Sn/C was evaluated in a direct ethanol fuel cell where Nafion 115 was used in the membrane electrodes assembly. The electrochemical analysis was carried out at 297 K. The electrocatalysts were homogeneously dispersed at a metal concentration of 0.4 mg·cm^{-2}. Carbon cloth was used in both electrodes as diffuser. The membrane electrodes assembly was prepared by hot pressing at 403 K and 100 kg·cm^{-2} for 5 min. The geometric area of the electrodes was 1 cm^2. 1 M reagent grade ethanol (J.T. Baker) was supplied in the anode of the fuel cell at a ratio of 1 $cm^3 \cdot min^{-1}$ and oxygen was supplied in the cathode at a ratio of 50 $cm^3 \cdot min^{-1}$.

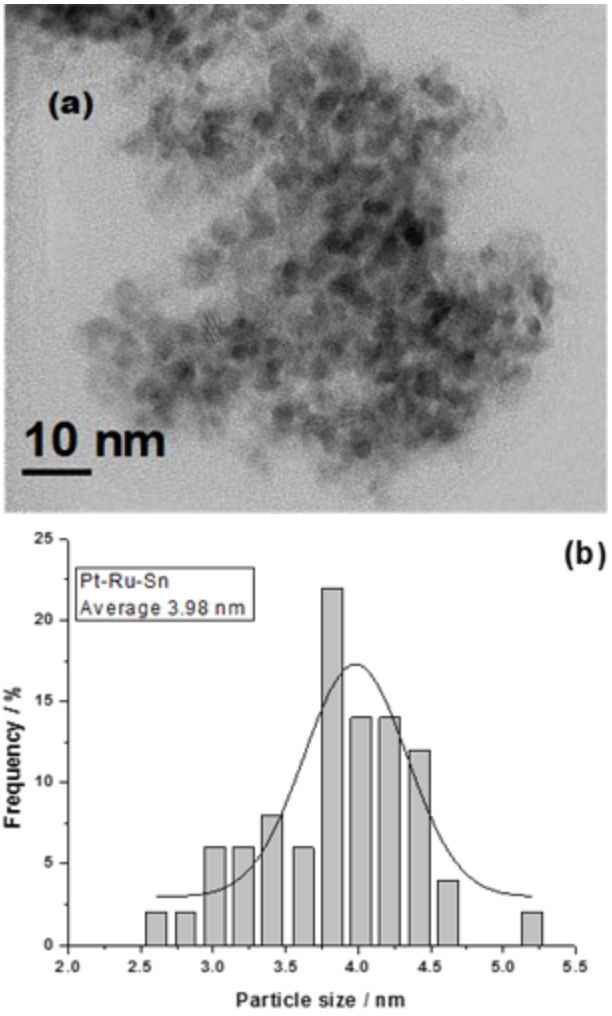

Figure 2. TEM image of the Pt-Ru-Sn system (**a**), the particle size distribution histogram (**b**).

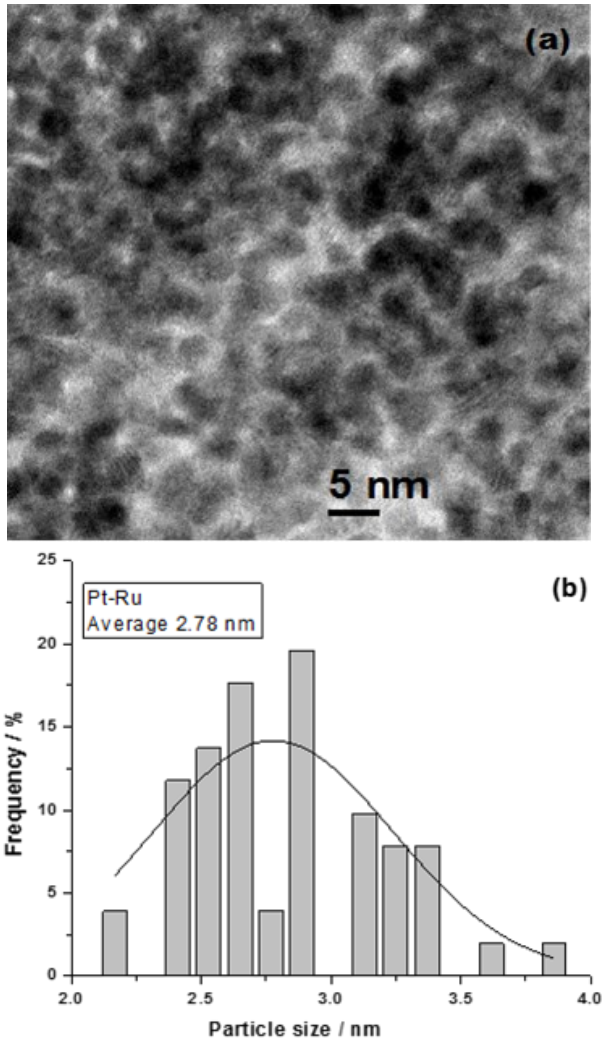

Figure 3. TEM image of the Pt-Ru system **(a)**, the particle size distribution histogram **(b)**.

3. RESULTS AND DISCUSSION

3.1. Structural characterization of electrocatalysts

In Figure 1 are shown the X-ray diffraction patterns of Pt-Ru-Sn/C, Pt-Ru/C and Pt-Sn/C. In the three systems, a peak at 2q close to 25º was associated to the (002) diffraction plane of the hexagonal structure of Carbon Vulcan XC-72R [4, 18]. Other diffraction peaks were also observed in all samples at 39, 46, 68, and 81º corresponding to (111), (200), (220) and (311) *fcc* Pt planes respectively (PDF card 04-08I2). For the case of Pt-Sn/C, it was observed a displacement to smaller values in the 2q position of the (111) plane corresponding to Pt. This shift was probably due to the incorporation of Sn into the crystal structure of Pt [19]. The diffractograms of Pt-Sn/C and Pt-Ru-Sn/C showed traces of SnO_2 by the presence of crystalline planes at 35 and 46 degrees. The formation of traces is probably due to the synthesis used for preparing the electrocatalysts. The presence of SnO_2 is not well understood in the electrocatalytic activity of Pt-Sn during the ethanol electrooxidation reaction. The diffraction peaks of Pt-Ru/C showed a shift to higher angle values than pure Pt, probably indicating the formation of an alloy between Pt and Ru [20, 21].

It was possible to estimate the crystal size of Pt-Sn/C, Pt-Ru/C and Pt-Ru-Sn/C using the Scherrer equation and the (111) plane [22]. The calculated crystal size was 2.27 nm for Pt-Ru/C, 2.28 nm for Pt-Sn/C and 2.63 nm for Pt-Ru-Sn/C. This result shows that the use of microwave assisted alcohol reduction process is an adequate method to synthesize binary or ternary nano-catalysts for electrochemical applications.

Particle size distribution of the nanoparticles was calculated by the analysis of TEM micrographs. Figure 2(a) shows a TEM image of the Pt-Ru-Sn/C sample. In Figure 2(b) is shown the particle size distribution of the Pt-Ru-Sn nanoparticles and it was observed a normal distribution around 3.98 nm mean particle size, which is in good agreement with the crystal size calculations obtained by XRD result. From our experience, Pt based electrocatalysts growing from 1 to 5 nm are adequate for alcohol electrooxidation reaction proba-

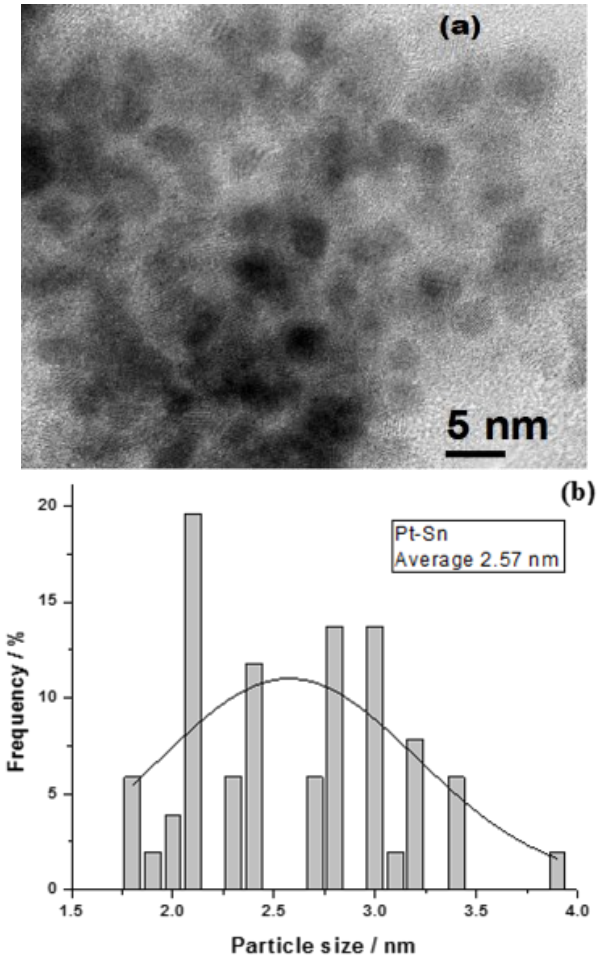

Figure 4. TEM image of the Pt-Sn system (**a**), the particle size distribution histogram (**b**).

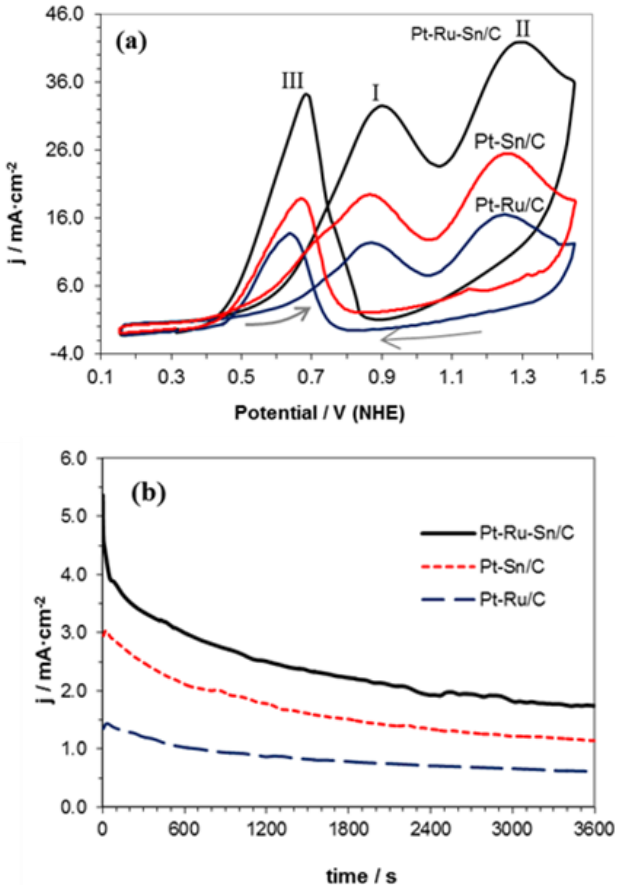

Figure 5. Cyclic voltammograms at 30 mV·s^{-1} scan rate for Pt-Ru-Sn/C, Pt-Sn/C and Pt-Ru/C (**a**), chronoamperograms at E = 0.55 V(NHE) in 0.5 M H_2SO_4+ 1 M of ethanol at temperature 298 K (**b**).

bly due to a surface area maximization of Pt in the matrix of the material. Figure 3 shows the TEM image of Pt-Ru/C. In Figure 3(a) is shown a typical image of semi-spherical Pt-Ru nanoparticles growing from 2.12 to 3.85 nm with a mean particle size ca. 2.7 nm (Figure 3(b)). The supporting method used in this work allowed the formation of well dispersed and controlled Pt-Ru nanoparticles. In Figure 4(a) is shown a TEM image of Pt-Sn/C nanoparticles. Semi-spherical nanoparticles are observed in the image with a mean particle size of 2.57 nm. The range of the nanoparticle size distribution was calculated between 1.8 to 3.9 nm (Figure 4(b)).

The specific surface area (SSA) of the electrocatalysts was calculated according to the relation established by $S = 6000 \cdot (D^* \rho)^{-1}$ [23]. A spherical morphology of the nanoparticles was assumed, D is the particle diameter (in nm) obtained from TEM micrographs and ρ is the density of Pt (21.4 g·cm^{-3}). The values of SSA were calculated for the three systems, obtaining 70.45, 100.85 and 109.10 m^{2}g^{-1} for the Pt-Ru/C, Pt-Sn/C and Pt-Ru-Sn/C respectively. The SSA value can be associated to the volumetric composition of bi-metallic or tri-metallic nanoparticles. It is expected that a higher value of SSA could correlate better electrochemical characteristics for ethanol electrooxidation.

3.2. Electrochemical characterization

The voltammograms at a scan rate of 30 mV·s^{-1} of the ethanol electro-oxidation reaction on Pt-Ru-Sn/C, Pt-Sn/C and Pt-Ru/C are shown in Figure 5(a). In the three systems, the catalytic load was 20% on a rotating disk electrode. The voltammograms of the three systems showed two oxidation peaks during the forward potential scan (I and II), and one re-oxidation peak (III) during the backward scan. The oxidation peak (I) is attributed to the complete ethanol electro-oxidation reaction with the formation of carbon dioxide. The oxidation peak (II) corresponds to the formation of acetaldehyde [12-13, 24-25]. The oxidation of the fuel in this case is associated to the chemisorption of oxygen species on the Pt surface. The re-oxidation peak (III) is a semi-quantitative parameter to evaluate the oxidation of intermediate species due to surface characteristics of the electrocatalysts [12-13, 24, 26-27]. Pt-Ru-Sn/C shows a catalytic surface more active than Pt-Sn/C and Pt-Ru/C, producing the highest values in current density at the same experimental conditions. There is a better distribution of Pt on the surface of the tri-metallic electrocatalyst than bi-metallic ones due to the presence of Ru and Sn. This results shows that for a catalytic system formed by Pt, Ru and Sn, a higher value in SSA contributes in better electro-

chemical characteristics for achieving the ethanol electro-oxidation reaction.

In Figure 5(b) are shown the chronoamperometric measurements of the three synthesized electrocatalysts at 0.55 V/NHE for 1 hr. The overpotential is higher than the ethanol oxidation threshold at the bi-metallic and tri-metallic electrocatalysts. Pt-Ru-Sn/C showed the highest dynamic current density associated to the ethanol electro-oxidation during 1 hr. The activity loss with respect to time for Pt-Ru/C is 2 times higher than Pt-Ru-Sn/C and for Pt-Sn/C is 0.75 times higher than the tri-metallic one. It is possible to consider that the interaction of oxophilic metals like Ru and Sn with Pt produces a weak CO bonding and a bifunctional mechanism more efficient than Pt-Ru/C and Pt-Sn/C at 297 K.

In Table 1 are summarized the kinetic parameters of the ethanol electro-oxidation on the three synthesized Pt based materials. According to these results, Pt-Ru-Sn/C showed the lowest onset potential (0.38 V/NHE) with respect to Pt-Sn/C and Pt-Ru/C (0.42 and 0.46 V/NHE respectively). The capability for oxidizing more completely CH_3CH_2OH to CO_2 is related to the potential E_I at the peak (I). A more positive value of E_I maximizes the possibility to complete the ethanol oxidation on the surface of the electrocatalysts. The potential E_I for Pt-Ru-Sn/C was observed at 0.9 V, and for Pt-Sn/C and Pt-Ru/C the E_I values were 0.88 and 0.87 V respectively. It means that the potential interval to complete the electrooxidation of ethanol shown by Pt-Ru-Sn/C is wider than Pt-Sn/C and Pt-Ru/C. The potentials are very similar in the three Pt based electrocatalysts for the partial electrooxidation of ethanol to produce acetaldehyde or acetic acid (E_{II}) as well as the re-oxidation (E_{III}). It means that the electrocatalytic routes have led to incomplete reactions of ethanol oxidation due to the catalytic nature of Pt independent of the binary or ternary electrocatalytic systems. The formation of incomplete reactions is independent of the metal used in binary or ternary electrocatalysts but the bifunctional mechanism is correlated to the metal used in the Pt based materials. The j_I/j_{II} ratio, (θ), is a qualitative parameter that represents the degree of ethanol to carbon dioxide conversion for this kind of electrocatalysts [28]. Pt-Ru-Sn/C showed the highest conversion with respect to Pt-Sn/C and Pt-Ru/C (0.81, 0.78 and 0.75 V/NHE respectively). The tri-metallic electrocatalyst showed better kinetic characteristics than Pt-Sn/C and Pt-Ru/C for the ethanol electro-oxidation. It is probably due to the interaction of Ru and Sn metallic and their oxide states with the hydroxyl species close to the catalytic surface immersed in the alcohol aqueous solution to promote a complete electro-oxidation of ethanol.

In figure 6 are shown the electrochemical impedance spectra of the synthesized electrocatalysts at a lower potential than the onset potential (0.30 V/NHE), and a potential where the complete electro-oxidation of ethanol has been carried out (0.55 V/NHE). In figure 6(a) are shown the impedance spectra at 0.30 V/NHE. It is

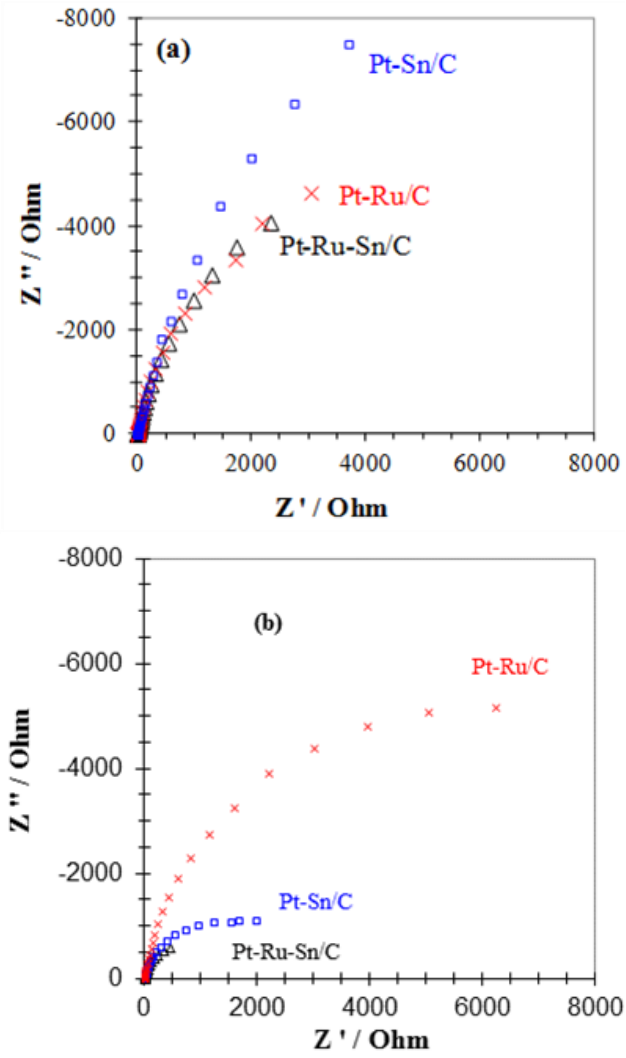

Figure 6. Nyquist diagrams of ethanol electro-oxidation reaction on Pt-Sn/C, Pt-Ru/C and Pt-Ru-Sn/C in 0.5 M H_2SO_4 + 1 M ethanol, (**a**) E=0.30 V/NHE and (**b**) E=0.55 V/NHE at 297 K.

observed that the three electrocatalyst systems have a similar performance, related to the charge transfer resistance in parallel to the double layer capacitance as has been previously discussed [22-23, 29-30]. At the condition of no ethanol electro-oxidation reaction, the calculated charge transfer resistances were 18.31, 18.89 and 11.27 kΩ-cm^2 for the Pt-Ru-Sn/C, Pt-Sn/C and Pt-Ru/C respectively. They are typical values for carbon-supported electrocatalysts in

Table 1. Kinetic parameters of the ethanol electro-oxidation reaction on the synthesized electrocatalysts.

Electrocatalysts	E_{onset} V	E_I V	$j_{(I)}$ mA·cm^{-2}	E_{II} V	$j_{(II)}$ mA·cm^{-2}	$E_{(III)}$ V	$j_{(III)}$ mA·cm^{-2}	(j_I/j_{II})
Pt-Ru-Sn/C	0.38	0.90	34.19	1.30	42.14	0.69	34.50	0.81
Pt-Sn/C	0.42	0.88	21.75	1.27	27.91	0.68	21.24	0.78
Pt-Ru/C	0.46	0.87	13.19	1.23	15.46	0.67	13.37	0.75

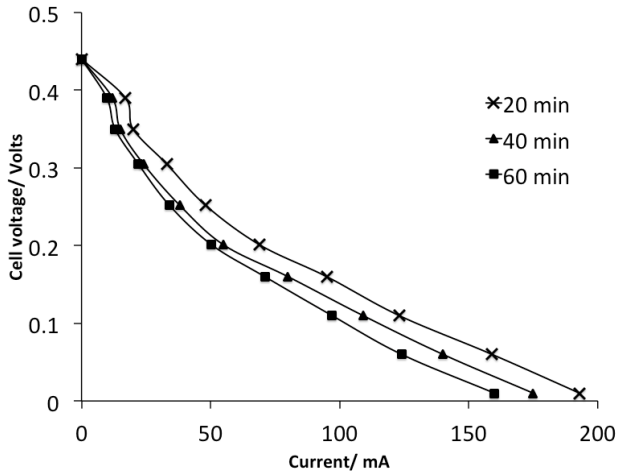

Figure 7. I-V Polarization and power density curves of a micro-direct ethanol fuel cell using Pt-Ru-Sn/C in the anode and Pt/C in the cathode. Experiments were carried out at 297 K.

aqueous systems. The electrochemical impedance response at 0.55 V/NHE changed significantly for the three systems (Figure 6(b)), Pt-Ru-Sn/C and Pt-Sn/C diminished their charge transfer resistance to 1.78 and 2.41 kΩ-cm^2 respectively, indicating the performance of the electrocatalysts during the ethanol electro-oxidation. In the case of Pt-Ru/C, its charge transfer resistance is still too high (10.29 kΩ-cm^2). It probably means that this electrocatalyst could have some adsorption problems with the formation of intermediate species during the entire process of the ethanol electro-oxidation.

3.3. DEFC single cell performance

Pt-Ru-Sn/C showed electrochemical characteristics better than Pt-Sn/C and Pt-Ru/C for ethanol electro-oxidation, so the ternary electrocatalyst was selected to be evaluated in an experimental DEFC. The result of power density of the DEFC is shown in Figure 7. The performance of the fuel cell using Pt-Ru-Sn/C in the anode was obtained at 297 K, the lowest temperature that has been reported for ethanol electro-oxidation in an experimental DEFC [31-34]. The open circuit voltage (V_{oc}) of the fuel cell was 430 mV and the short circuit current (I_{SC}) was 1.92 mA·cm^{-2}. The maximum electrical power was 0.14 mW·cm^{-2}. After 1 hr of fuel cell operation, the I_{SC} diminished 16% and the V_{oc} remained at the same value. There was no change in the ohmic resistance of the cell during 1 hr of fuel cell operation at 297 K, so the variation in current density as a function of time in the DEFC could be associated to the alcohol crossover from the anode to cathode of the fuel cell or by depleting ethanol species at the anode side of the fuel cell.

4. CONCLUSION

Pt-Ru-Sn/C and related bimetallic systems as Pt-Ru/C and Pt-Sn/C were synthesized by microwave assisted alcohol-reduction method. The mean particle size in all systems was less than 10 nm indicating the success of the synthesis method used for preparing electrocatalysts. The ternary material based in Pt-Ru-Sn/C showed better characteristics for the ethanol electro-oxidation than bimetallic ones due to the inclusion of Ru and Sn in the Pt matrix. The presence of Sn and Ru forming the ternary system improved the ethanol electro-oxidation due to the affinity of those metals with hydroxyl species to complete the electro-oxidation reaction. The inclusion of Ru and Sn associated to the main electrocatalyst diminished the charge transfer resistance to complete the ethanol electro-oxidation as it was discussed in the impedance analysis of the electrocatalytic systems. The results obtained from the evaluation of Pt-Ru-Sn/C as anodic electrocatalyst in a micro direct ethanol fuel cell showed the feasibility of using the synthesized material in experimental fuel cells for oxidizing complex alcohols.

5. ACKNOWLEDGMENTS

Authors like to thank Mrs. Maria Luisa Ramon Garcia for the XRD characterization and discussion of results and Mr. Gildardo Casarrubias Segura for sample preparations. Mr. Carlos Flores Morales, Dr. Hilda Esparza Ponce and Dr. Jose Alvaro Chavez Carvayar, for their support for the samples characterization by TEM. Authors are also grateful to CONACYT Grants 128545 and DGAPA PAPIIT IN111011 to develop and support this project. CONACYT Ph.D. scholarship 212785 for Francisco Ginez is appreciated.

REFERENCES

[1] Antoniassi R.M, Silva J. C. M, Oliveira Neto A, Spinacé E.V., Appl. Catal., B., 254, 120 (2017).
[2] Chu, Y. H. Shul, Y. G, Int. J. Hydrogen Energy, 35, 11261 (2010).
[3] Badwal, S. P. S., Giddey, S., Kulkarni, A., Goel, J., Basu, S., Appl. Energy, 145, 80 (2010).
[4] Antoniassi, R. M., Oliveira Neto, A., Linardi, M, Spinacé, E. V., Int. J. Hydrogen Energy, 38, 12069 (2013).
[5] Chen, F., Ren, J, He, Q., Liu, J, Song, R., J. Colloid Interface Sci., 497, 276 (2017).
[6] Narayanamoorthy, B., Datta, K. K. R., Eswaramoorthy, M, Balaji, S., ACS Catal., 4, 3621 (2014).
[7] Li, S., Hui X., Zhiping X, Ke Z, Caiqin W, Bo Y, Jun G, Yukou D. *Appl. Surf. Sci.,* 422, 172 (2017).
[8] El Jawad, M. K., Gilles, B, Maillard, F., Key Eng. Mater., 735, 219 (2017).
[9] Tao, J. ping , Qing-shuang Ji, Gui-fang Shao, Ze-peng Li, Tun-dong Liu, Yu-hua Wen, *J. Alloys Compd.,* 716, 240 (2017).
[10]Aoki, N. Inouea H., Shiraib, A., Higuchib,S., Matsuib,Y., Daimonb H., Doib T., Inaba, M. Electrochim. Acta, 244, 146 (2017).
[11]Dong H, Dong L., Inorg. Organomet. Polym., 21, 754 (2011).
[12]Nakagawa N, Kaneda Y, Wagatsuma M, Tsjiguchi T, J. Power Sources, 199, 103 (2012).
[13]García G, Tsiouvaras N, Pastor E, Peña AM, Fierro GJL, Martínez-Huerta VM, Int. J. Hydrogen Energy, 37, 7131 (2012).
[14]Ribadeneira E, Hoyos AB, J. Power Sources, 180, 238 (2008).
[15]Oliveira NA, Dias RR, Tusi MM, Linardi M, Spinacé VE, J. Power Sources, 166, 87 (2007).
[16]Spinacé VE, Oliveira NA, Vasconcelos TRR, Linardi M, J.

Power Sources, 137, 17 (2004).
[17]Chen WX, Lee JY, Liu Z, Chem. Commun., 2588 (2002).
[18]Li L, Huang M, Liu J, Guo Y, J. Power Sources., 196, 1090 (2011).
[19]Ma Y, Wang H, Ji S, Linkov V, Wang R, J. Power Sources, 247, 142 (2014).
[20]Guo L, Chen S, Li L, Wei Z, J. Power Sources, 247, 360 (2014).
[21]Zou L, Guo J, Liu J, Zou Z, Akins LD, Yang H, J. Power Sources, 248, 356 (2014).
[22]Barreto BC, Parreira LTR, Goncalves RR, De Azevedo CD, Fritz Huguenin, J. Power Sources, 185, 6 (2008).
[23]Guo J.W, Zhao T.S, Prabhuram J, Wong C.C, Electrochimica Acta, 50, 1973 (2005).
[24]Wang H, Jusys Z, Behn RJ, J. Power Sources, 154, 351 (2006).
[25]Fujiwuara N, Friedrich KA, Stimming U., J. Electroanal. Chem., 472, 120 (1999).
[26]Razmi H, Habibi Es, Heidari H, Electrochim Acta, 53, 8178 (2008).
[27]Shao MH, Adzic RR, Electrochim. Acta, 50, 2415 (2005).
[28]Wang MY, Chen JH, Fan Z, Tang H, Deng GH, He DL, Kuang YF, Carbon, 42, 3257 (2004).
[29]Hoa LQ, Vestergaard MC, Yoshikawa H, Saito M, Tamiya E, Electrochemistry Communications, 13, 746 (2011).
[30]Wongyao N, Therdthianwong A, Therdthianwong S, Energy Conversion and Management, 52, 2676 (2011).
[31]Tayal J, Rawat B, Basu S, Int. J. Hydrogen Energy, 37, 4597 (2012).
[32]Battirola LC, Schneider JF, Torriani ICL, Tremiliosi-Filho G, Rodrigues-Filho UP, Int. J. Hydrogen Energy, 38, 12060 (2013).
[33]Chu HY, Shul GY, Int. J. Hydrogen Energy, 35, 11261 (2010).
[34]Rousseau S, Coutanceau C, Lamy C, Léger J-L, J. Power Sources, 158, 18 (2006).